

Metal–coumarin complexes: synthesis and characterization of 7-isocyanocoumarin ligands and $\text{Mo}(\text{CO})_4(7\text{-isocyanocoumarin})_2$ complexes. X-ray crystal structure of $\text{Mo}(\text{CO})_4(7\text{-isocyano-4-trifluoromethylcoumarin})_2$

Daniel A. Freedman*, Ivan Keresztes, Ann L. Asbury

Department of Chemistry, State University of New York at New Paltz, New Paltz, NY 12561, USA

Received 11 June 2001; accepted 3 August 2001

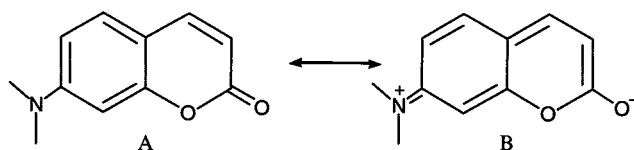
Abstract

The preparation and characterization of four different 7-isocyanocoumarin ligands is described. The four ligands are 3,4-dimethyl-7-isocyanocoumarin (Dmic), 7-isocyano-4-methylcoumarin (Mic), 3-chloro-7-isocyano-4-methylcoumarin (Cmic) and 7-isocyano-4-trifluoromethylcoumarin (Tic). Reaction of the four 7-isocyanocoumarin ligands with $\text{Mo}(\text{CO})_4(\text{pip})_2$ (pip = piperidine) gave the $\text{Mo}(\text{CO})_4\text{L}_2$ complexes. IR and UV–vis spectra of the complexes indicate that the 7-isocyanocoumarin ligands are significantly stronger π -acids than simple aromatic isocyanide ligands. An intense visible absorption band, assigned to a metal-to-ligand charge transfer (MLCT) transition, is present in the UV–vis spectra of the four $\text{Mo}(\text{CO})_4\text{L}_2$ complexes. Excitation into the MLCT band of the Mic, Cmic, and Dmic complexes gave yellow–orange emission at room temperature in methylene chloride solution. Photolysis of $\text{Mo}(\text{CO})_4(\text{Mic})_2$ with $\text{P}(\text{Ph})_3$ in THF solution produced $\text{Mo}(\text{CO})_3(\text{PPh}_3)(\text{Mic})_2$. © 2002 Elsevier Science B.V. All rights reserved.

Keywords: Molybdenum; Isocyanide; Coumarin; Photochemistry

1. Introduction

Coumarin and its derivatives have attracted interest in several fields. Our interest is in the properties of metal–coumarin complexes, a subject which has received relatively little attention. Outside of natural products chemistry [1], the interest in coumarins is due mainly to their interesting photochemical and photo-physical properties [2,3]. The most pertinent example is the intense tunable, visible wavelength emission displayed by 7-aminocoumarins. Emission from 7-aminocoumarins is thought to occur from the lowest singlet excited state which has been described as an intramolecular charge transfer (ICT) transition and can be represented by resonance structure B shown below, where charge from the amine has been transferred to the unsaturated lactone ring [4].



The charge-transfer nature of the 7-aminocoumarin excited state suggests that metal–coumarin complexes could display interesting excited state properties. Considerable effort in recent years has gone towards the design of metal–ligand complexes that display photo-induced charge separation, a key process in designing artificial photosynthetic systems, chemical sensors, and molecular level devices [5]. A particular goal is to prepare complexes which have low energy metal-to-ligand charge transfer (MLCT) excited states. There are only a few examples in the literature of metal–coumarin complexes. Koefod and Mann prepared $[\text{CpRu}(7\text{-aminocoumarin})]^+$ complexes where the metal is coordinated in η^6 fashion to the arene portion of the 7-aminocoumarin [6]. An intense visible absorption band was observed in these complexes assigned to a

* Corresponding author.

E-mail address: freedman@newpaltz.edu (D.A. Freedman).

Ru → coumarin charge transfer transition. Puddephat and Aye reported the preparation of Pt(Bpy)(Me)₂Br(4-CH₂-7-methoxycoumarin) where the Pt is bonded to the coumarin methyl group [7]. More recently, Tyson and Castellano prepared ruthenium complexes of a phenanthroline ligand with a pendant coumarin group [8]. Our interest is in complexes with direct conjugation between the coumarin and the metal, which is lacking the latter two examples. The presence of charge-transfer absorbance bands in the [CpRu(7-aminocoumarin)]⁺ complexes suggests that the ruthenium is strongly conjugated with the coumarin moiety and that further investigation of metal–coumarin complexes is warranted. However, it would be useful to have a more versatile ligating group on the coumarin than the arene ring. Our strategy is to prepare isocyanocoumarin ligands

An isocyanocoumarin should be an excellent ligand. Isocyanides in general act as both σ -donors and π -acids making them capable of stabilizing metals in a wide range of oxidation states [9]. In addition, metal–arylisocyanide complexes have been shown to have interesting photochemical and photophysical properties indicative of strong conjugation between the metal and the isocyanide ligand [10–14]. The work reported here describes the preparation of 7-isocyanocoumarin ligands and Mo(CO)₄(7-isocyanocoumarin)₂ complexes. The molybdenum complexes were chosen because they are readily prepared and there are data available in the literature on analogous complexes of simple aryl and alkyl isocyanide complexes [13,14].

2. Experimental

2.1. General considerations

Mo(CO)₄(pip)₂ [15] (pip = piperidine), Mo(CO)₄(Dmp)₂ [16], and 7-aminocoumarins [17] were prepared via literature procedures. Mo(CO)₆, ethylacetoacetate, ethyl 2-methylacetoacetate, ethyl 2-chloroacetoacetate, and ethyl 4,4,4-trifluoroacetoacetate were purchased from Aldrich Chemical Co. 2,6-Dimethylphenylisocyanide was purchased from Fluka. [Ru(bpy)₃]Cl₂ was purchased from Aldrich and metathesized to the hexafluorophosphate salt by adding NH₄PF₆ to an aqueous solution of [Ru(bpy)₃]Cl₂. The [Ru(bpy)₃][PF₆]₂ was purified by chromatography (alumina–acetonitrile), recrystallized from CH₃CN–Et₂O and dried in vacuo. All synthetic procedures were carried out under an inert N₂ atmosphere unless otherwise noted. CH₂Cl₂ was distilled from P₂O₅. THF was distilled from Na–benzophenone. Acetonitrile was distilled from P₂O₅. Toluene was reagent grade and was used without further purification. ¹H-NMR spectra were recorded on JEOL 90FXQ and Varian 300 spectrometers. Chemical

shifts are relative to (CH₃)₄Si. UV–vis spectra were recorded in non-degassed solutions at room temperature (r.t.) with a Cary 1 spectrometer. Elemental analyses were performed by MHW Laboratories.

2.2. Emission studies

Solutions of Mo(CO)₄(7-isocyanocoumarin)₂ complexes were prepared in the dark. Emission spectra were recorded on an Ocean Optics S2000 CCD Array fiber optic spectrometer. Excitation at 405 nm was provided by a 200 W mercury vapor lamp using the appropriate interference filter. Emission from the sample was focused on to the fiber optic cable with a fiber-optic focusing assembly (Oriel). A 475 nm cut-off filter was placed over the focusing assembly to prevent interference from the excitation line. Optically dense solutions ($A > 10$ in a 1.0 cm cell at the excitation wavelength) of the complexes were prepared from freshly distilled methylene chloride and purged with argon for 15 min. Emission was detected from the front face. The emission spectra were corrected for grating efficiency and detector response. The values of Φ_{em} were determined from relative peak areas using a solution of [Ru(bpy)₃][PF₆]₂ ($\Phi_{em} = 0.068$) as a standard [18]. Optically dense solutions of [Ru(bpy)₃][PF₆]₂ were prepared from freshly distilled acetonitrile and purged with argon for 15 min. Corrections were made for differences in the refractive indices of the solvents [18].

2.3. 7-Formamido-4-methylcoumarin (Mfc)

7-Amino-4-methylcoumarin (4.5 g, 0.026 mol), 40 ml of toluene and 20 ml of 88% formic acid were added to a round bottom flask equipped with a stir bar, Dean–Stark trap and a reflux condenser. The mixture was refluxed for 14 h during which time the water formed in the reaction was collected in the Dean–Stark trap as the water–toluene azeotrope. After 14 h, the excess formic acid was distilled off. The solution was cooled, precipitating the product which was filtered and washed with diethyl ether giving 4.22 g (79.9% yield) of off-white powder. ¹H-NMR (90 MHz, *d*₆-DMSO): 2.41 (s, CH₃), 6.26 (s, H³), 7.2–7.8 (m, H^{5,6,8}), 8.39 (s, HCO *Z* isomer), 9.01 (d, HCO *E* isomer, $J = 10.8$ Hz), 10.58 (d, HN *E* isomer, $J = 9.9$ Hz), 11.02 (s, HN *Z* isomer).

2.4. 3,4-Dimethyl-7-formamidocoumarin (Dmfc)

3,4-Dimethyl-7-aminocoumarin (4.12 g, 0.0218 mol) was treated in the same manner as 7-amino-4-methylcoumarin giving 2.5 g (53% yield) of off-white powder. ¹H-NMR (90 MHz, *d*₆-DMSO): 2.08 (s, CH₃), 2.35 (s, CH₃), 7.0–7.8 (m, H^{5,6,8}), 8.36 (s, HCO *Z* isomer), 9.0 (s, HCO *E* isomer), 10.50 (s, HN *E* isomer), 10.76 (s, HN *Z* isomer).

2.5. 3-Chloro-4-methyl-7-formamidocoumarin (Cmfc)

7-Amino-3-chloro-4-methylcoumarin (2.0 g, 0.0095 mol) was treated in the same manner as 7-amino-4-methylcoumarin giving 2.14 g (95% yield) of off-white powder. ¹H-NMR (90 MHz, *d*₆-DMSO): 2.53 (s, CH₃), 7.1–8.0 (m, H^{5,6,8}), 8.38 (s, HCO *Z* isomer), 9.01 (d, HCO *E* isomer, *J* = 9.9 Hz), 10.42 (broad s, HN *E* isomer), 10.65 (s, HN *Z* isomer).

2.6. 7-Formamido-4-trifluoromethylcoumarin (Tfc)

7-Amino-4-trifluoromethylcoumarin (4.0 g, 0.017 mol) was treated in the same manner as 7-amino-4-methylcoumarin giving 3.75 g (86% yield) of light yellow powder. ¹H-NMR (90 MHz, *d*₆-DMSO): 6.92 (s, H³), 7.2–8.0 (m, H^{5,6,8} *E* and *Z* isomers), 8.42 (s, HCO *Z* isomer), 9.07 (d, HCO *E* isomer, *J* = 10.5 Hz), 10.65 (d, HN *E* isomer, *J* = 10.4 Hz), 10.80 (s, HN *Z* isomer).

2.7. 7-Isocyano-4-methylcoumarin (Mic)

7-Formamido-4-methylcoumarin (2.8 g, 0.014 mol) was added to 20 ml of methylene chloride and stirred to form a slurry. Triethylamine (9.5 ml, 0.069 mol) was added to the flask through a short column of activated alumina. Phosphorous oxychloride (1.3 ml, 0.014 mol) was added dropwise by syringe. The reaction was stirred for 30 min, during which time the formamide completely dissolved leaving a clear yellow solution. The reaction mixture was extracted with 2 × 10 ml portions of water and once with 10 ml of saturated NaCl solution. The methylene chloride layer was dried with anhydrous MgSO₄ and suction filtered through 5 cm of silica gel in a fritted funnel. The solvent was removed via rotary evaporation giving the product as an off-white powder which was dried in vacuo (1.8 g, 69% yield). The crude product was suitable for synthesis. Chromatography on silica gel, eluting with methylene chloride, gave analytically pure material. ¹H-NMR (300 MHz, CD₂Cl₂): 2.48 (m, CH₃), 6.32 (q, H³, *J*_{3-Me} = 1.2 Hz), 7.34 (apparent s, H⁸), 7.33 (d of d, H⁶, *J*₆₋₅ = 9.0 Hz, *J*₆₋₈ = 2.0 Hz), 7.65 (d, H⁵, *J*₅₋₆ = 8.1 Hz).

2.8. 3,4-Dimethyl-7-isocyanocoumarin (Dmic)

3,4-Dimethyl-7-formamidocoumarin (1.5 g, 0.0069 mol) was treated in the same manner as 7-formamido-4-methylcoumarin giving 0.90 g (65% yield) of colorless powder. ¹H-NMR (300 MHz, CD₂Cl₂): 2.40 (s, CH₃⁴), 2.20 (s, CH₃³), 7.31 (m, H^{6,8}), 7.64 (H⁵, d, *J*₅₋₆ = 9.0 Hz).

2.9. 3-Chloro-4-methyl-7-isocyanocoumarin (Cmic)

3-Chloro-7-formamido-4-methylcoumarin (2.0 g, 0.0084 mol) was treated in the same manner as 7-formamido-4-methylcoumarin giving 1.1 g (60% yield) of white powder. ¹H-NMR (300 MHz, CD₂Cl₂): 2.63 (s, CH₃), 7.43 (m, H⁸), 7.38 (m, H⁶), 7.69 (m, H⁵).

2.10. 7-Isocyano-4-trifluoromethylcoumarin (Tic)

7-Formamido-4-trifluoromethylcoumarin (2.0 g, 0.0078 mol) was treated in the same manner as 7-formamido-4-methylcoumarin giving 1.5 g (80% yield) of light yellow powder. ¹H-NMR (300 MHz, CD₂Cl₂): 6.87 (q, H³, *J*_{3-CF₃} = 0.8 Hz), 7.34 (apparent s, H⁸), 7.38 (d of d, H⁶, *J*₆₋₅ = 8.6 Hz, *J*₆₋₈ = 2.0 Hz), 7.78 (d of q, H⁵, *J*₅₋₆ = 8.6 Hz, *J*_{5-CF₃} = 1.8 Hz).

2.11. Mo(CO)₄(Mic)₂

Mo(pip)₂(CO)₄ (0.100 g, 0.347 mmol) and Mic (0.141 g, 0.760 mmol) were added to a three necked flask equipped with a reflux condenser and a stir bar. Freshly distilled methylene chloride (20 ml) was added and the solution was purged with N₂. The solution was refluxed for 2 h. The resulting orange solution was cooled and CH₃OH was added until the solution turned cloudy. After 18 h at –15 °C, the resulting precipitate was filtered and washed with diethyl ether giving an orange, microcrystalline product (0.095 g, 48% yield). Slow recrystallization in the dark from CH₂Cl₂–hexane gave analytically pure material. Further purification for absorption–emission spectroscopy studies was accomplished by chromatography on silica gel, eluting with methylene chloride. The pure product eluted first as a yellow–orange band followed by a red band. The product was isolated by adding hexanes to the methylene chloride solution, precipitating the product as a yellow powder. ¹H-NMR (300 MHz, CD₂Cl₂): 2.43 (d, CH₃, *J*_{CH₃-3} = 1.0 Hz), 6.30 (apparent d, H³, *J*_{3-CF₃} = 1.0 Hz), 7.33 (d, H⁸), 7.32 (d of d, H⁶, *J*₆₋₅ = 9.0 Hz, *J*₆₋₈ = 2.0 Hz), 7.66 (d, H⁵, *J*₅₋₆ = 9.0 Hz).

2.12. Mo(CO)₄(Dmic)₂

Mo(pip)₂(CO)₄ (0.0937 g, 0.325 mmol) and Dmic (0.144 g, 0.723 mmol) were treated in a similar manner as above to give orange microcrystals (0.121 g, 61.4% yield). A yellow powder was isolated after chromatography. ¹H-NMR (300 MHz, CD₂Cl₂): 2.40 (s, CH₃⁴), 2.20 (s, CH₃³), 7.30 (d, H⁸, *J*₈₋₆ = 2.0 Hz), 7.31 (d of d, H⁶, *J*₆₋₅ = 9.0 Hz, *J*₆₋₈ = 2.0 Hz), 7.65 (d, H⁵, *J*₅₋₆ = 9.3 Hz).

2.13. $\text{Mo}(\text{CO})_4(\text{Cmic})_2$

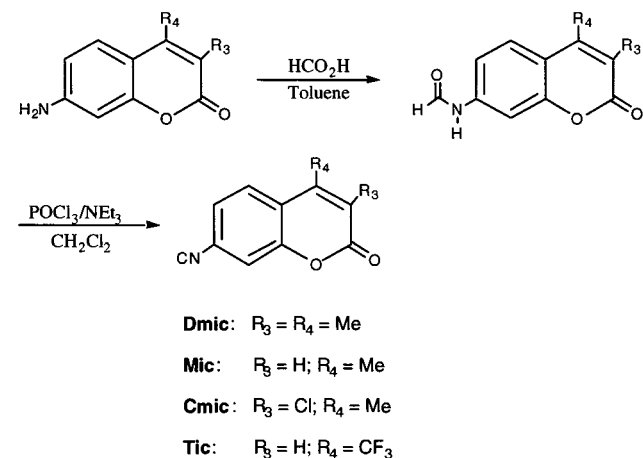
$\text{Mo}(\text{pip})_2(\text{CO})_4$ (0.100 g, 0.347 mmol) and Cmic (0.168 g, 0.763 mmol) were treated in a similar manner as above to give reddish–orange microcrystals (0.137 g, 61.0% yield). An orange powder was isolated after chromatography. $^1\text{H-NMR}$ (300 MHz, CD_2Cl_2): 2.59 (s, CH_3), 7.36 (d, H^8 , $J_{8-6} = 2.0$ Hz), 7.36 (d of d, H^6 , $J_{6-5} = 9.0$ Hz, $J_{6-8} = 2.0$ Hz), 7.70 (d, H^5 , $J_{5-6} = 9.0$ Hz).

2.14. $\text{Mo}(\text{CO})_4(\text{Tic})_2$

$\text{Mo}(\text{pip})_2(\text{CO})_4$ (0.200 g, 0.529 mmol) and Tic (0.278 g, 1.16 mmol) were added to a three necked flask equipped with a reflux condenser and a stir bar. Freshly distilled methylene chloride (20 ml) was added and the solution was purged with N_2 . The solution was refluxed for 2 h, changing color from light yellow to dark red. The solvent was removed via rotary evaporation and the resulting red solid was dried in vacuo. The solid was dissolved in CH_3OH and cooled at -15 °C for 2 weeks giving an analytically pure mixture of dark red powder and needles (0.060 g, 16.5% yield). $^1\text{H-NMR}$ (300 MHz, CD_2Cl_2): 6.84 (s, H^3), 7.39 (m, $\text{H}^{6,8}$), 7.77 (d, H^5 , $J_{5-6} = 8.4$ Hz).

2.15. $\text{Mo}(\text{Mic})_2(\text{CO})_3\text{PPh}_3$

$\text{Mo}(\text{Mic})_2(\text{CO})_4$ (60.0 mg, 0.130 mmol), triphenylphosphine (34.1 mg, 0.13 mmol) and 10 ml of freshly distilled THF were added to a Pyrex tube equipped with a stir bar. The tube was connected to a vacuum line and the orange solution was freeze-pump-thaw degassed (three cycles). The solution was photolyzed for 2 h with a 175 W medium pressure Hg lamp giving a dark red solution. The THF was removed under reduced pressure leaving a dark red residue which was



Scheme 1.

dissolved in CH_2Cl_2 . Adding hexanes precipitated a dark red powder (60 mg, 57% yield). Slow recrystallization from CH_2Cl_2 –hexanes gave analytically pure product. IR (CH_2Cl_2); ν_{CO} (cm^{-1}) = 1905 (s), 1941 (m), 1965 (sh), $\nu_{\text{CN}} = 2006$ (s), 2096 (w); ν_{lactone} (cm^{-1}) = 1732 (m), 1606 (s).

2.16. X-ray crystal structure determination for $\text{Mo}(\text{CO})_4(\text{Tic})_2$

Dark red needles of $\text{Mo}(\text{CO})_4(\text{Tic})_2$ were grown by cooling a CH_3OH solution of the complex to -15 °C (Table 4). A crystal of the compound was attached to a glass fiber and mounted on the Siemens SMART system for a data collection at 173(2) K. An initial set of cell constants was calculated from reflections harvested from three sets of 30 frames. These initial sets of frames are oriented such that orthogonal wedges of reciprocal space were surveyed. This produces orientation matrices determined from 91 reflections. Final cell constants are calculated from a set of 5478 strong reflections from the actual data collection. The data were collected by the hemisphere collection method where a randomly oriented region of reciprocal space is surveyed to the extent of 1.3 hemispheres to a resolution of 0.84 Å. Three major swaths of frames are collected with 0.30° steps in ω .

The space group $Pnma$ was determined based on systematic absences and intensity statistics. A successful direct-methods solution was calculated which provided most non-hydrogen atoms from the R -map. Several full-matrix least squares-difference Fourier cycles were performed which located the remainder of the non-hydrogen atoms. All non-hydrogen atoms were refined with anisotropic displacement parameters unless stated otherwise. All hydrogen atoms were placed in ideal positions and refined as riding atoms with individual (or group if appropriate) isotropic displacement parameters.

The sample was collected with 30 s frames, because the sample was small. One half of the complex is in the asymmetric unit: the Mo atom and two carbonyl ligands are located on the crystallographic mirror.

3. Results

3.1. Ligand synthesis and characterization

7-Aminocoumarins can be prepared via a literature procedure [17] and provide a convenient starting material for the preparation of 7-isocyanocoumarins. The 7-isocyanocoumarins are prepared from the 7-aminocoumarins as shown in Scheme 1. Refluxing the 7-aminocoumarins in formic acid–toluene produced the 7-formamidocoumarins. The 7-formamidocoumarins

Table 1
Analytical data for 7-formylcoumarins, 7-isocyanocoumarins, and Mo(CO)₄(7-isocyanocoumarin)₂ complexes

	Formula	Calculated (%)			Experimental (%)		
		C	H	N	C	H	N
Tfc	C ₁₁ H ₆ F ₃ NO ₃	51.38	2.35	5.45	51.30	2.30	5.53
Mfc	C ₁₂ H ₁₁ NO ₃	65.02	4.46	6.89	64.78	4.69	6.93
Mic	C ₁₁ H ₇ NO ₂	71.34	3.82	7.57	71.52	4.00	7.33
Dmic	C ₁₂ H ₉ NO ₂	72.35	4.55	7.03	72.43	4.37	7.05
Cmic	C ₁₁ H ₆ ClNO ₂	60.16	2.75	6.38	60.32	2.50	6.22
Tic	C ₁₁ H ₄ F ₃ NO ₂	55.24	1.69	5.87	55.60	2.12	5.64
Mo(CO) ₄ (Mic) ₂	C ₂₆ H ₁₄ MoN ₂ O ₈	54.00	2.44	4.84	54.16	2.60	4.60
Mo(CO) ₄ (Dmic) ₂	C ₂₈ H ₁₈ MoN ₂ O ₈	55.46	2.99	4.61	55.62	3.06	4.49
Mo(CO) ₄ (Cmic) ₂	C ₂₆ H ₁₂ Cl ₂ MoN ₂ O ₈	48.25	1.87	4.33	47.44	1.96	4.11
Mo(CO) ₄ (Tic) ₂	C ₂₆ H ₈ F ₆ MoN ₂ O ₈	45.50	1.17	4.08	45.60	1.22	3.83
Mo(CO) ₃ (Mic) ₂ PPh ₃	C ₄₃ H ₂₉ MoN ₂ O ₇ P	63.56	3.60	3.45	63.80	3.88	3.45

Table 2
IR data (cm⁻¹) for 7-isocyanocoumarin ligands and Mo(CO)₄L₂ complexes

	$\nu(\text{CN})$	$\nu(\text{lactone})$				
Dmic	2123 (m)	1713 (s), 1614 (m)				
Mic	2128 (m)	1732 (s), 1614 (m)				
Cmic	2127 (m)	1738 (s), 1606 (m)				
Tic	2131 (m)	1753 (s), 1616 (m)				
	$\nu(\text{CN})$		$\nu(\text{CO})$	$\Delta(\text{CN})^b$		
Mo(CO) ₄ (Dmic) ₂	2136 (w)	2079 (m)	2068(sh)	2014 (m)	1940 (s)	-44
Mo(CO) ₄ (Mic) ₂	2135 (w)	2077 (m)	2059(sh)	2012(m)	1941 (s)	-51
Mo(CO) ₄ (Cmic) ₂	2134 (w)	2067 (m)	2087 (sh)	2012 (m)	1943 (s)	-60
Mo(CO) ₄ (Tic) ₂	2135 (w)	2067 (m)	2051(sh)	2012 (m)	1945 (s)	-64
Mo(CO) ₄ (Dmpi) ₂	2138 (w)	2094 (m)	^a	2016 (m)	1932 (s)	-26

All data were acquired in CH₂Cl₂ solution.

^a Not observed.

^b See text for explanation.

were characterized by ¹H-NMR spectroscopy and by elemental analysis (Table 1) for Tfc and Mfc. The ¹H-NMR spectra are similar for all four formamides. The resonances for the coumarin ring protons are complex due to small chemical shift differences for the aromatic hydrogens and the presence of two different formamide isomers. The presence of two formamide isomers is typical, and is caused by restricted rotation about the C–N bond [19]. The isomer is designated *E* when the NH and formyl hydrogens are *trans* and *Z* when the hydrogens are *cis*. Although the signals for the aromatic protons are too complex to readily interpret, two signals each are observed for the formyl and NH hydrogen resonances in ca. a 3:1 ratio, clearly showing the presence of the two isomers. Coupling between the NH and formyl protons is observed only for the minor isomer. Since the coupling constant should be greater when the formyl and NH protons are *trans*, the predominant isomer is assigned the *Z* configuration and the minor the *E* configuration.

Dehydration of the formamides to the isocyanides is readily accomplished with phosphorous oxychloride using a modification of a literature procedure [20]. Four different isocyanocoumarins, designated Dmic, Mic, Cmic, and Tic, were prepared with different substituents in the three and four positions. Purification by column chromatography yielded either colorless (Mic, Dmic, Cmic) or pale yellow (Tic) products which gave acceptable elemental analyses (Table 1). The 7-isocyanocoumarins were stable when stored at -15 °C, but exhibited substantial decomposition over several weeks at room temperature. None of the unpleasant odor associated with more volatile isocyanides was observed.

The 7-isocyanocoumarins were fully characterized by ¹H-NMR, IR, and UV–vis spectroscopy. The ¹H-NMR spectra are similar to those reported for other coumarins [17]. The solution IR spectra (Table 2) of the 7-isocyanocoumarins exhibit three peaks of interest. The peak at ca. 2130 cm⁻¹ is assigned to the CN stretch of the isocyanide group. Small variations in the

position of this band are observed for the four different isocyanides, but there does not appear to be any obvious correlation with the coumarin substituents. Two peaks in the 1600–1750 cm^{-1} region are assigned to the ν_{CO} and $\nu_{\text{C}=\text{C}}$ stretches of the vinyl lactone ring. The band assigned to the C=C stretch exhibits almost no variation in position, while the C=O stretch shows the expected correlation with the coumarin substituents, shifting from 1713 cm^{-1} (Dmic) to 1753 cm^{-1} (Tic).

The UV–vis spectra of the 7-isocyanocoumarins were investigated in methylene chloride solution (Fig. 1). The UV–vis spectra of the four ligands are similar, exhibiting a peak at about 320 nm which has an intense high energy shoulder and a weak low energy shoulder, and two narrower, more intense bands centered at ca. 280 nm. The only significant deviation from this general pattern occurs for Tic for which the high energy shoulder on the 320 nm peak is not observed and the lower energy of the two narrow, higher energy bands appears as a shoulder rather than as a separate peak. The features observed in the spectra of the 7-isocyanocoumarins have similar energies and relative intensities to the spectrum of coumarin itself. Coumarin exhibits intense UV–vis peaks at 310, 285, 274, and 220 nm

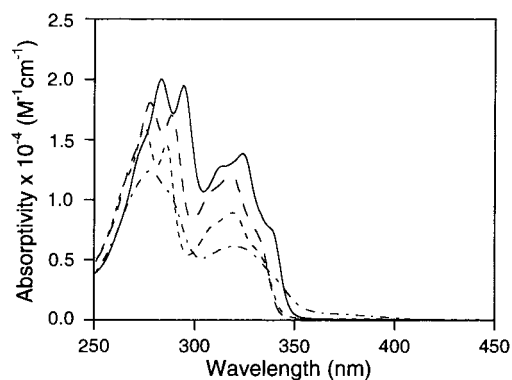


Fig. 1. UV–vis spectra of Cmic (—); Dmic(---); Mic (-.-), and Tic (· · ·) in CH_2Cl_2 solution.

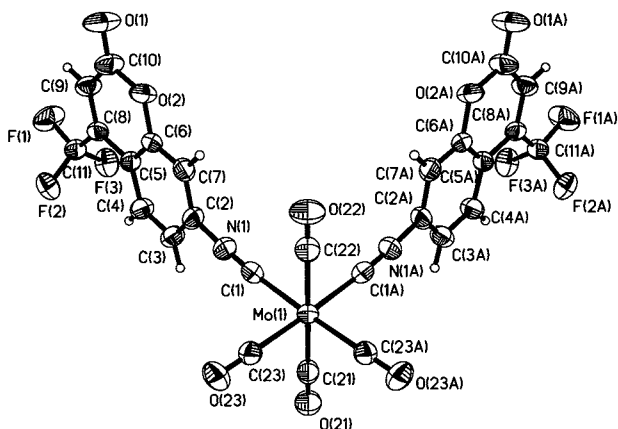


Fig. 2. ORTEP view of $\text{Mo}(\text{CO})_4(\text{Tic})_2$.

which have been assigned to $\pi-\pi^*$ transitions [21]. INDO calculations indicate that a forbidden $n-\pi^*$ transition could also be present at longer wavelengths. This feature was not observed for coumarin itself, but is commonly observed in substituted coumarins. The similarity between the spectra of the 7-isocyanocoumarins and coumarin suggest that the four intense, higher energy features can be assigned to $\pi-\pi^*$ transitions, and the weak, low energy shoulder on the ca. 320 nm band can be assigned to an $n-\pi^*$ transition. The latter assignment is supported by the consistent shift of this band to lower energy as the coumarin substituents become more electron withdrawing.

3.2. Synthesis and characterization of $\text{Mo}(\text{CO})_4\text{L}_2$ complexes

The $\text{Mo}(\text{CO})_4(7\text{-isocyanocoumarin})_2$ complexes were prepared by refluxing $\text{Mo}(\text{CO})_4(\text{pip})_2$ (pip = piperidine) with the isocyanide ligand in methylene chloride solution [15]. The complexes were recrystallized from $\text{CH}_2\text{Cl}_2\text{-MeOH}$ to eliminate piperidine then a second time from $\text{CH}_2\text{Cl}_2\text{-hexanes}$ to give products with acceptable elemental analyses (Table 1). An exception to this was $\text{Mo}(\text{CO})_4(\text{Tic})_2$ which crystallized out of a cold methanol solution as analytically pure material, albeit in poor yield. The four compounds range in color from yellow (Mic and Dmic complexes) to orange (Cmic complex) to red (Tic complex). The compounds were stable as solids and in solution when protected from light. Further purification for UV–vis absorption and emission studies was necessary for all compounds except for $\text{Mo}(\text{CO})_4(\text{Tic})_2$. This was accomplished by chromatography on silica gel, eluting with methylene chloride, to eliminate small amounts of the $\text{Mo}(\text{CO})_3(7\text{-isocyanocoumarin})_3$ complexes present as contaminants.

We were able to obtain needles of $\text{Mo}(\text{CO})_4(\text{Tic})_2$ suitable for X-ray analysis by cooling a methanol solution of the complex. The ORTEP (Fig. 2) of a single molecule shows that the Tic ligands are in the *cis* conformation with ca. octahedral geometry about the molybdenum. There is a mirror plane bisecting the angle between the isocyanide ligands, giving the molecule C_s symmetry. The bond angles are quite close to the expected 90° with the largest deviation being the angle between the two isocyanide ligands at 86.2° (Table 5). The isocyanides show only a slight deviation from linearity with CNC bond angles of 176.2° . The carbonyl carbons are closer to the metal than the isocyanide carbons by an average of 0.076 \AA . The Mo–CO bonds are about 0.030 \AA shorter for carbonyls *trans* to an isocyanide compared to a carbonyl *trans* to another carbonyl, consistent with the greater σ donating ability of the isocyanide vs. carbonyl ligands. The C(22)–Mo(1)–C(2)–C(7) dihedral angle is 5.93° , indicat-

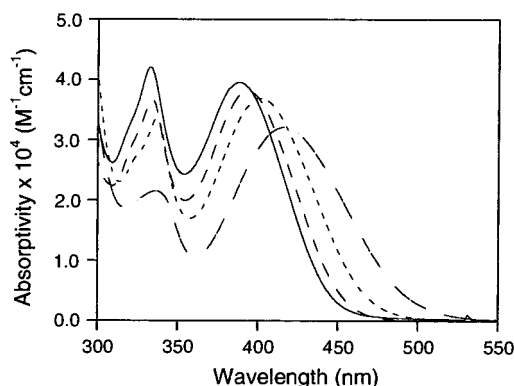


Fig. 3. UV-vis spectra of $\text{Mo}(\text{CO})_4(\text{Dmic})_2$ (—), $\text{Mo}(\text{CO})_4(\text{Mic})_2$ (---), $\text{Mo}(\text{CO})_4(\text{Cmic})_2$ (-.-), and $\text{Mo}(\text{CO})_4(\text{Tic})_2$ (- - -) in CH_2Cl_2 solution.

Table 3

UV-vis absorption (λ_{max} in nm (ϵ in $\text{cm}^{-1} \text{M}^{-1} \times 10^4$)) and emission spectral data for 7-isocyanocoumarin and $\text{Mo}(\text{CO})_4(7\text{-isocyanocoumarin})_2$ compounds^a

	Absorption		Emission	
	MLCT	$\pi-\pi^*$	λ_{max}	$\Phi_{\text{em}}^{\text{e}}$
Dmic	^b	318 (1.20)		
Mic	^b	319 (0.89)		
Cmic	^b	324 (1.39)		
Tic	^b	320 (0.61)		
$\text{Mo}(\text{CO})_4(\text{Dmic})_2$	388 (3.96)	333 (4.21)	649	0.0016
$\text{Mo}(\text{CO})_4(\text{Mic})_2$	394 (3.81)	334 (3.67)	617	0.0024
$\text{Mo}(\text{CO})_4(\text{Cmic})_2$	401 (3.69)	337 (3.36)	626	0.0048
$\text{Mo}(\text{CO})_4(\text{Tic})_2$	416 (3.21)	336 (2.15)		
$\text{Mo}(\text{CO})_4(\text{Tic})_2^{\text{c}}$	397 (3.21)	335 (2.70)		
$\text{Mo}(\text{CO})_4(\text{Tic})_2^{\text{d}}$	413 (3.13)	338 (2.05)		
$\text{Mo}(\text{CO})_4(\text{Tic})_2^{\text{e}}$	423	337		
$\text{Mo}(\text{CO})_3(\text{Mic})_2\text{PPh}_3^{\text{f}}$	429	337		

^a All data were acquired in methylene chloride solution unless otherwise noted. Extinction coefficients were determined from the peak maxima and are not corrected for overlapping bands.

^b Not observed.

^c Recorded in acetone.

^d Recorded in toluene.

^e Recorded in 10% toluene-hexanes.

^f Recorded in THF.

^g Error for Φ_{em} values is $\pm 10\%$.

ing that the coumarin ligand is tilted slightly away from being parallel with the mirror plane. The other coumarin ring is tilted to the same degree with the CF_3 groups on the two 7-isocyanocoumarins pointing away from one another.

The $\text{Mo}(\text{CO})_4(7\text{-isocyanocoumarin})_2$ complexes were also characterized by $^1\text{H-NMR}$, IR, and UV-vis spectroscopy. The $^1\text{H-NMR}$ spectra of the compounds are very similar to the spectra of the free ligands, showing almost no chemical shift differences between the signals for the complexed and free ligands. Examination of the IR spectra of the $\text{Mo}(\text{CO})_4\text{L}_2$ complexes (Table 2) in

methylene chloride solution reveals four main peaks in the CO and CN stretching region at ca. 2135, 2070, 2012, and 1940 cm^{-1} . The assignments in Table 2 were made by comparison with the reported IR spectrum of $\text{Mo}(\text{CO})_4(\text{Dmp})_2$ (Dmp = 2,6-dimethylphenylisocyanide) [16b]. The IR bands generally show only a small dependence on the isocyanocoumarin ligand. An exception to this is the lower energy of the two isocyanide CN stretches, which shifts from 2067 cm^{-1} in $\text{Mo}(\text{CO})_4(\text{Tic})_2$ to 2079 cm^{-1} for $\text{Mo}(\text{CO})_4(\text{Dmic})_2$.

The UV-vis spectra of the four $\text{Mo}(\text{CO})_4\text{L}_2$ complexes were investigated in methylene chloride solution (Fig. 3; Table 3). All four complexes exhibit four intense absorption bands: two narrow bands between 269 and 296 nm, a band at ca. 335 nm which displays a high energy shoulder, and a broad, intense absorbance that ranges between 388 nm for the Dmic complex and 416 nm for the Tic complex. The spectrum of $\text{Mo}(\text{CO})_4(\text{Tic})_2$ was also investigated in different solvents; the lowest energy band exhibited considerable solvatochromism, shifting from 397 nm in acetone solu-

Table 4

Crystal data and structure refinement parameters for $\text{Mo}(\text{CO})_4(\text{Tic})_2$

Empirical formula	$\text{C}_{13}\text{H}_4\text{F}_3\text{Mo}_{0.50}\text{NO}_4$
Formula weight	343.14
Temperature (K)	173(2)
Wavelength (\AA)	0.71073
Crystal system	Orthorhombic
Space group	<i>Pnma</i>
Unit cell dimensions	
<i>a</i> (\AA)	13.5633(7)
<i>b</i> (\AA)	31.190(2)
<i>c</i> (\AA)	6.0041(3)
α ($^\circ$)	90
β ($^\circ$)	90
γ ($^\circ$)	90
<i>V</i> (\AA^3)	2539.9(2)
<i>Z</i>	8
<i>D</i> _{calc} (mg m^{-3})	1.795
Absorption coefficient (mm^{-1})	0.616
<i>F</i> (000)	1352
Crystal size (mm)	$0.42 \times 0.16 \times 0.03$
θ range for data collection ($^\circ$)	1.31–25.10
Index ranges	$-12 \leq h \leq 16$, $-33 \leq k \leq 37$, $-7 \leq l \leq 7$
Reflections collected	12167
Independent reflections	2294 ($R_{\text{int}} = 0.0660$)
Absorption correction	Semi-empirical
Max/min. transmission	0.63 and 0.55
Refinement method	Full-matrix least-squares on F^2
Data/restraints/parameters	2293/0/206
Goodness-of-fit on F^2	1.293
Final <i>R</i> indices [$I > 2\sigma(I)$]	$R_1 = 0.0643^{\text{a}}$, $wR_2 = 0.1428^{\text{b}}$
<i>R</i> indices (all data)	$R_1 = 0.0756$, $wR_2 = 0.1490$
Largest difference peak and hole (e \AA^{-3})	0.669 and -1.527

$$^{\text{a}} R_1 = \frac{\sum ||F_o| - |F_c||}{\sum |F_o|}$$

$$^{\text{b}} wR_2 = \sqrt{\frac{\sum w(F_o^2 - F_c^2)^2}{\sum wF_o^4}}$$

Table 5
Selected bond lengths (Å) and angles (°) for Mo(CO)₄(Tic)₂

<i>Bond lengths</i>	
Mo(1)–C(1)	2.116(5)
C(1)–N(1)	1.159(6)
Mo(1)–C(23)	2.023(5)
C(23)–O(23)	1.147(6)
Mo(1)–C(22)	2.057(8)
C(22)–O(22)	1.133(9)
Mo(1)–C(21)	2.058(8)
C(21)–O(21)	1.143(9)
<i>Bond angles</i>	
C(23)–Mo(1)–C(23)	88.9(3)
C(23)–Mo(1)–C(22)	90.7(2)
C(23)–Mo(1)–C(21)	90.9(2)
C(23)–Mo(1)–C(1)	92.4(2)
C(22)–Mo(1)–C(1)	87.4(2)
C(21)–Mo(1)–C(1)	90.9(2)
C(1)–Mo(1)–C(1)	86.2(3)
N(1)–C(1)–Mo(1)	176.4(4)

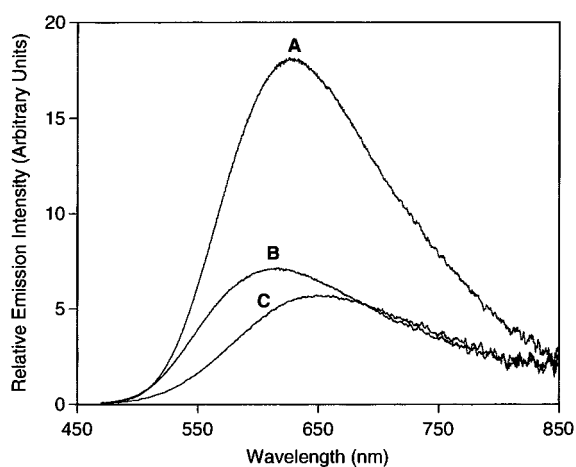


Fig. 4. Corrected emission spectra of Mo(CO)₄(Cmic)₂ (A); Mo(CO)₄(Mic)₂ (B); and Mo(CO)₄(Dmic)₂ (C) in CH₂Cl₂ solution.

tion to 423 nm in 10% toluene–hexane. The higher energy band at ca. 335 nm shows essentially no solvent dependence. Several of the higher energy features are readily assigned by comparison with the spectra of the ligands. With the exception of the Tic complex, the two sharp, high-energy bands are nearly identical in both wavelength and general appearance to peaks in the spectra of the ligands and are thus assigned to intra-ligand transitions. These bands in the Tic complex shift about 10 nm to shorter wavelengths relative to the free ligand, but retain the same general appearance. The bands at ca. 335 nm also have a very similar appearance to ligand bands, but are shifted 10–15 nm to longer wavelengths. The shift is large for a ligand centered transition, but the lack of any solvatochromic behavior combined with the similarity in appearance of

this band between the free and complexed ligands leads us to assign this to an intra-ligand transition. It is likely that the π bonding and antibonding orbitals of the isocyanide group are involved in the ligand π – π^* transitions, so it is not surprising that complexation of the ligand to the metal should cause some shift in certain π – π^* transitions. The lowest energy band is clearly not ligand centered. The wavelength of this band shows a significant dependence on the coumarin substitution, following the trend Mo(CO)₄(Dmic)₂ < Mo(CO)₄(Mic)₂ < Mo(CO)₄(Cmic)₂ < Mo(CO)₄(Tic)₂. Clearly, as the ligand substituents become more electron withdrawing the band shifts to longer wavelength. This suggests that this band is a Mo \rightarrow coumarin charge transfer transition. The solvatochromism supports this assignment. The band shifts to longer wavelengths in less polar solvents, consistent with the solvatochromic behavior of the MLCT bands observed in the analogous molybdenum and tungsten complexes of mono- and bidentate pyridine ligands [22].

The emission spectra of the Mo(CO)₄L₂ complexes were investigated at room temperature in methylene chloride solution. The L = Dmic, Mic, and Cmic, complexes exhibited a broad and unstructured emission profile (Fig. 4; Table 3) upon excitation into the MLCT absorbance band. No emission was observed from Mo(CO)₄(Tic)₂. The emission maxima are 617, 626 and 649 nm for the Mic, Cmic, and Dmic complexes, respectively. Emission quantum yields were determined for the three complexes and are given in Table 3.

3.3. Photochemistry of Mo(CO)₄(Mic)₂

Photolysis of a THF solution of Mo(CO)₄(Mic)₂ and PPh₃ results in a color change from orange to red. A dark red powder was isolated from the solution which, after recrystallization from CH₂Cl₂–hexanes, analyzed well for Mo(CO)₃(PPh₃)(Mic)₂. The UV–vis spectrum of this complex shows a broad band at 427 nm and a sharper band at 337 nm assigned to MLCT and intra-ligand transitions, respectively. The MLCT transition is shifted to longer wavelengths compared to Mo(CO)₄(Mic)₂ by the increase in electron density at the metal due to the substitution of a phosphine for CO. In comparison, the 337 nm band is identical in position and appearance to the analogous band in Mo(CO)₄(Mic)₂, consistent with it being a ligand centered transition. Photolysis of the Mo(CO)₄L₂ complexes in methylene chloride in the absence of a ligand also leads to decomposition. We are currently investigating the products of the reaction, but preliminary experiments suggest that a ligand disproportionation reaction is occurring as was observed for Mo(CO)₃(CNCF₃)₃ [23].

4. Discussion

The spectroscopic characteristics of the $\text{Mo}(\text{CO})_4\text{L}_2$ complexes of the 7-isocyanocoumarin ligands are qualitatively similar to the analogous complexes of simple arylisocyanide ligands, but we observed spectral shifts showing that the coumarin moiety enhances the electron withdrawing ability of the isocyanide ligand. In the IR this results in enhanced $\text{Mo} \rightarrow \text{CNR}$ backbonding as measured by the shift in the CN stretching frequency between the free and complexed isocyanides (Table 2). For instance, the decrease in the CN stretching frequency is only -26 cm^{-1} for $\text{Mo}(\text{CO})_4(\text{Dmpi})_2$ (Dmpi = 2,6-dimethylphenylisocyanide). A much larger shift is observed for the 7-isocyanocoumarin ligands, ranging from -44 cm^{-1} for Dmic to -64 cm^{-1} for Tic, showing the expected correlation with the electron donating–withdrawing properties of the coumarin substituents. In the UV–vis spectra, the greater electron accepting ability of the 7-isocyanocoumarin ligands versus simple aryl isocyanide ligands is manifested in the significant red shift of the MLCT transitions for the isocyanocoumarin complexes. The MLCT bands for the 7-isocyanocoumarin complexes range from 388 nm for the Dmic complex to 416 nm for the Tic complex. In comparison, the MLCT bands for the analogous complexes of Dmpi, *p*-Me- $\text{C}_6\text{H}_4\text{CN}$ [14], and *p*-Cl- $\text{C}_6\text{H}_4\text{CN}$ [14] are at 358, 360 and 367 nm, respectively.

The room temperature emission observed from the 7-isocyanocoumarin complexes is assigned to be of MLCT origin. The emission is not due to the presence of small amounts of the free ligands since the ligands do not exhibit any visible wavelength emission. The low energy of the emission maxima as well as the broad, unstructured appearance of the emission bands are very similar to the MLCT emission observed for the analogous $\text{Mo}(\text{CO})_4(\text{py})_2$ (py = substituted pyridine) complexes [22a]. The emission maxima of the Mic and Cmic complexes are in the expected order with the presence of the chlorine shifting the emission to lower energy. Surprisingly, the Dmic complex exhibits the longest wavelength emission of the three complexes. This suggests that there is a greater degree of distortion in the excited state of this complex, but it is not apparent why this should be the case.

In comparison to the intense emission observed from the 7-isocyanocoumarin complexes, no emission is observed at room temperature for $\text{Mo}(\text{CO})_4(\text{Dmpi})_2$, even though an MLCT band is present in the absorbance spectrum. This is probably due to efficient non-radiative decay from LF excited states that are at energies lower than or similar to the energy of the MLCT state. Metal–carbonyl complexes typically do not exhibit room temperature emission due to rapid CO dissociation from LF excited states. The carbonyl

complexes which do exhibit room temperature emission typically have MLCT excited states which are lower in energy than the LF states [24]. One relevant example here is the series of $\text{Mo}(\text{CO})_4(\text{py})_2$ complexes studied by Lees et al. Two main absorbance bands are observed for these compounds. The higher energy bands, (350–385 nm) are assigned to LF transitions and the lower energy bands (395–468 nm) are assigned to MLCT transitions. Room temperature emission is observed for all of these compounds. Comparison to the isocyanide complexes is interesting. We were not able to observe LF bands for any of the isocyanide complexes, but it is likely that they will not be shifted significantly relative to the pyridine complexes because of the consistent effect of the four carbonyl ligands. This would place the LF bands for $\text{Mo}(\text{CO})_4(\text{Dmpi})_2$ near the MLCT band (358 nm). In comparison, the MLCT bands for the 7-isocyanocoumarin complexes are shifted to wavelengths very similar to the MLCT bands observed for the pyridine complexes. Since the LF bands should remain largely unshifted, the MLCT state is now lower in energy and radiative deactivation from the MLCT state then becomes competitive with non-radiative relaxation from the LF states.

5. Conclusions

We have synthesized four different 7-isocyanocoumarin ligands substituted in the three and four positions and $\text{Mo}(\text{CO})_4(7\text{-isocyanocoumarin})_2$ complexes of the four ligands. The X-ray crystal structure of $\text{Mo}(\text{CO})_4(\text{Tic})_2$ demonstrates that the 7-isocyanocoumarin ligands are in the *cis* configuration with essentially octahedral geometry about the metal. The UV–vis and IR data are consistent with the expectation that the 7-isocyanocoumarin ligands are significantly stronger π -acids than simple arylisocyanide ligands. Presumably this is due to coupling of the low energy π^* orbitals of the coumarin to the molybdenum through the CN bridge. Comparison of the complexes of the four different ligands shows that the electronic properties of the 7-isocyanocoumarin ligands can be ‘tuned’ by varying the coumarin substituents. The $\text{Mo}(\text{CO})_4\text{L}_2$ complexes of the 7-isocyanocoumarin complexes exhibit emission at room temperature in fluid solution. This is a rare property for metal–carbonyl complexes and is probably due to the presence of the relatively low energy MLCT excited states. Our future work will concentrate on further characterizing the metal–coumarin excited states for molybdenum and other metals. Additionally, we plan to investigate the interaction of metal–coumarin complexes with nucleic acids.

6. Supplementary material

Crystallographic data for the structural analysis have been deposited with the Cambridge Crystallographic Data Centre, CCDC no. 164518 for compound $\text{Mo}(\text{CO})_4(\text{Tic})_2$. Copies of this information may be obtained free of charge from The Director, CCDC, 12 Union Road, Cambridge CB2 1EZ, UK (Fax: +44-1223-336033; e-mail: deposit@ccdc.cam.ac.uk or www: <http://www.ccdc.cam.ac.uk>).

Acknowledgements

We thank The Research Corporation for their generous support of this research. We thank Dr Kent Mann for numerous helpful discussions. We thank Dr Victor G. Young, Jr. and the University of Minnesota X-ray Crystallographic Laboratory for solving the crystal structure of $\text{Mo}(\text{CO})_4(\text{Tic})_2$.

References

- [1] Robert Murray, Jesus Mendez, Stewart Brown, *The Natural Coumarins: Occurrence, Chemistry, and Biochemistry*, Wiley, New York, 1982.
- [2] N.J. Turro, *Modern Molecular Photochemistry*, Benjamin/Cummings, Menlo Park, CA, 1978, p. 462.
- [3] George G. Chimino, Howard B. Gamper, Stephen T. Isaacs, John E. Hearst, *Ann. Rev. Biochem.* 54 (1985) 1151 and references therein.
- [4] K.H. Drexhage, *Dye lasers*, in: F.P. Schafer (Ed.), *Topics in Applied Physics 1*, Springer-Verlag, West Berlin, 1973 Chapter 4.
- [5] See for example: (a) V. Balzani, F. Scandola, *Supramolecular Photochemistry*, Ellis Horwood, New York, 1991; (b) V. Balzani, A. Juris, M. Venturi, *Chem. Rev.* 96 (1996) 759; (c) T.J. Meyer, *Acc. Chem. Res.* 22 (1989) 163.
- [6] (a) R.S. Koefod, K.R. Mann, *Inorg. Chem.* 28 (1989) 2285; (b) R.S. Koefod, K.R. Mann, *Inorg. Chem.* 30 (1991) 2221.
- [7] K. Aye, R.J. Puddephatt, *Inorg. Chim. Acta* 235 (1995) 307.
- [8] Daniel S. Tyson, Felix N. Castellano, *Inorg. Chem.* 38 (1999) 4382.
- [9] (a) M.P. Guy, J.T. Guy, D.W. Bennett, *J. Mol. Struct.* 122 (1985) 95; (b) L. Malatesta, F. Bonati, *Isocyanide Complexes of Metals*, Wiley, New York, 1969; (c) J.A.S. Howell, J. Saillard, A. Le Beuze, G. Jaouen, *J. Chem. Soc. Dalton* (1982) 2533.
- [10] (a) K.R. Mann, M. Cimolino, G.L. Geoffrey, G.S. Hammond, A.A. Orio, G. Albertin, H.B. Gray, *Inorg. Chim. Acta* 16 (1976) 97; (b) K.R. Mann, H.B. Gray, G.S. Hammond, *J. Am. Chem. Soc.* 99 (1977) 306; (c) H.B. Gray, K.R. Mann, N.S. Lewis, J.A. Thich, R.M. Richman, *Inorganic and organometallic photochemistry*, in: M.S. Wrighton (Ed.), *Advances in Chemistry Series 168*, American Chemical Society, Washington, DC, 1978, p. 44.
- [11] (a) N.E. Stacy, K.A. Connor, D.R. McMillin, R.A. Walton, *Inorg. Chem.* 25 (1986) 3649; (b) C.J. Cameron, S.M. Tetrick, R.A. Walton, *Organometallics* 3 (1984) 240.
- [12] J.E. Larowe, D.R. McMillin, N.E. Stacy, S.M. Tetrick, R.A. Walton, *Inorg. Chem.* 26 (1987) 966.
- [13] J.A. Connor, E.M. Jones, G.K. McEwen, M.K. Lloyd, J.A. McCleverty, *J. Chem. Soc. Dalton* (1972) 1246.
- [14] R.W. Balk, D.J. Stufkens, A. Oskam, *Inorg. Chim. Acta* 48 (1981) 105.
- [15] D.J. Darensbourg, R.L. Kump, *Inorg. Chem.* 17 (1978) 2680.
- [16] (a) N.J. Coville, M.O. Albers, *Inorg. Chim. Acta* 65 (1982) L7; (b) M. Minelli, W. Maley, *J. Inorg. Chem.* 28 (1989) 2954.
- [17] L. Ronald Atkins, E. Dan Bliss, *J. Org. Chem.* 43 (1978) 1975.
- [18] Hai Sun, Z. Morton Hoffman, *J. Phys. Chem.* 97 (1993) 11956.
- [19] W.E. Stewart, T.H. Siddall, *Chem. Rev.* 70 (1970) 517.
- [20] L.H. Tietze, T. Eicher, *Reactions and Synthesis in the Organic Chemistry Laboratory*, University Science Books, Mill Valley, CA, 1989, p. 486.
- [21] R.H. Abu-Eittah, B.A. El-Tawil, *Can. J. Chem.* 63 (1985) 1173.
- [22] (a) S. Chun, E.E. Getty, A.J. Lees, *Inorg. Chem.* 23 (1984) 2155; (b) D.M. Manuta, A.J. Lees, *Inorg. Chem.* 25 (1986) 1354; (c) H.B. Abrahamson, M.S. Wrighton, *Inorg. Chem.* (1978) 3385.
- [23] Dieter Lentz, *J. Organomet. Chem.* 381 (1990) 205.
- [24] A.J. Lees, *Chem. Rev.* 87 (1987) 711.